Aluminum protection by using green zirconium oxide layer and organic coating: an efficient and adherent dual system

Vitor B. Moreira,[1,2] Alvaro Meneguzzi,[2] Emilio Jiménez-Piqué,[3,4] Carlos Alemán,[1,4]

Elaine Armelin [1,4,]*

[1] Departament d'Enginyeria Química, Universitat Politècnica de Catalunya, Campus Diagonal Besòs (EEBE), C/ Eduard Maristany, 10-14, Building I, 2nd floor, 08019, Barcelona, Spain; vitor.moreira@upc.edu; carlos.aleman@upc.edu; elaine.armelin@upc.edu

[2] Programa de Pós-graduação em Engenharia de Minas, Metalúrgica e de Materiais (PPGE3M), Universidade Federal do Rio Grande do Sul (UFRGS), Av. Bento Gonçalves, 9500 – 91501-970, Porto Alegre, RS, Brazil; meneguzzi@ufrgs.br

[3] Department of Materials Science and Engineering, Universitat Politècnica de Catalunya, Campus Diagonal Besòs - EEBE, C/ Eduard Maristany, 10-14, Building I, 1st floor, 08019, Barcelona, Spain; emilio.jimenez@upc.edu

[4] Barcelona Research Center for Multiscale Science and Engineering, Universitat Politècnica de Catalunya, Campus Diagonal Besòs (EEBE), C/ Eduard Maristany, 10-14, Building I, basement floor, 08019, Barcelona, Spain; emilio.jimenez@upc.edu; carlos.aleman@upc.edu; elaine.armelin@upc.edu

***Corresponding authors*: elaine.armelin@upc.edu**

2. Experimental section

2.1. Materials

The composition analysis of aluminum substrates is provided. AA1100 is a commercially pure Al class (in wt. %): Cu (0.34); Fe (0.42); Si (0.19); Mn (<0.01); Ti (<0.02); Zn (<0.01) and balanced Al. The chemical composition was provided by the supplier (Irmãos Galeazi Ltda., Brazil). The AA2024-T3 is the structural reinforced Cu-rich grade with metallurgical temper code T3, which is referred to solution heat treated, cold worked and naturally aged. The AA2024 panel has chemical composition of (in wt. %): Cu (4.63); Mg (1.66); Mn (0.55); Fe (0.36); Si (0.31); and balanced to Al. The compositional analysis for this alloy was determined by ICP-AES (spectrometer SPECTROMAXx).

3. Results and Discussion

3.1. The stability of ZrO_2 nanocoating comparing the DC and EAD deposition methods

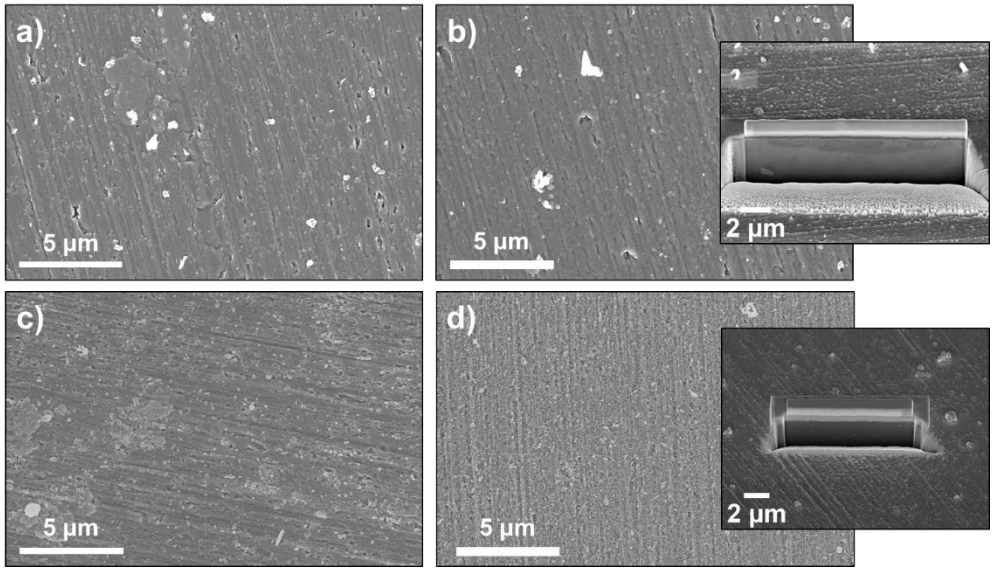

Figure S1. Topography SEM images of: a) AA1100/Zr-DC coating; b) AA1100/Zr-EAD coating; c) AA2024/Zr-DC coating; and d) AA2024/Zr-EAD coating. The insets on b) and d) images represent the cross-cut of those sample surfaces (by focused ion beam), used for the thicknesses measurements.

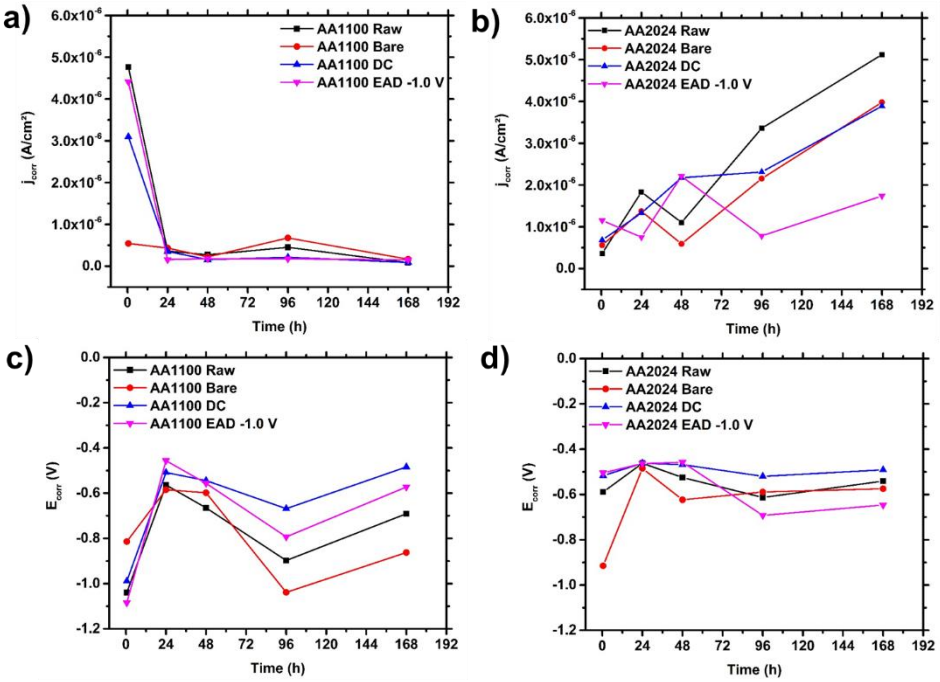

Figure S2. Corrosion current densities (J_{corr}) measured on: a) AA1100 and b) AA2024 substrates; and corrosion potentials (E_{corr}) measured on: c) AA1100 and d) AA2024 treated specimens. The values correspond to the Tafel extrapolation of the polarization curves obtained during the exposure of the analyzed samples to a NaCl 0.05M electrolyte, throughout 168 h (7 days).

3.2. Porosity and barrier properties of Zr-EAD and Zr-CCC coatings evaluated by potentiodynamic polarization curves, EIS analysis and accelerated corrosion test

The Nyquist plots (Figures S3a and S4a) are mainly represented by a single time constant behavior corresponding to the electrical equivalent circuit (EEC) of $R_s(R_pCPE_{dl})$, where R_s represents the ohmic resistance of electrolyte solution, R_p is the polarization resistance of the interface cladding, and CPE_{dl} corresponds to the double-layer constant phase element of a non-ideal capacitor, when the phase angle is different from −90°.

In Figure S3, the Nyquist and Bode plots of initial and final immersion times are reported. After 168 h of test, it may be observed that all the AA1100 specimens suffered a slight reduction of their resistive property, if compared to the first immersion step (24h). Considering that the sample AA1100 Zr-DC is the one that had the less pronounced

change throughout the test, there is a possibility that the pseudo-barrier protection provided by the ZrO_2 film partially avoids the growth of the Al_2O_3 layer. The Zr-DC cladding resulted in the highest impedance values after 168 h of analysis.

Contrasting with the observed impedance response of AA1100 alloy, it is noticeable in Figure S4 that all the AA2024 samples had a decrease in the impedance values throughout the test duration and a second time constant appeared at low frequencies.

At the conclusion of the test, as seen in Figure S4 (a1-b1), the Zr-EAD sample provided the best protection to the substrate, with increased exposure time. Thus, AA2024 Zr-EAD seems to have a more stable, more uniform and more compact film, as observed by SEM (Figure S1). Unlike the AA1100 alloy, it is evident that in Cu-rich alloy, whose native oxide layer does not provide a satisfactory barrier protection, the production of ZrO_2 by EAD method generates a more efficient barrier able to diminish electrolyte penetration.

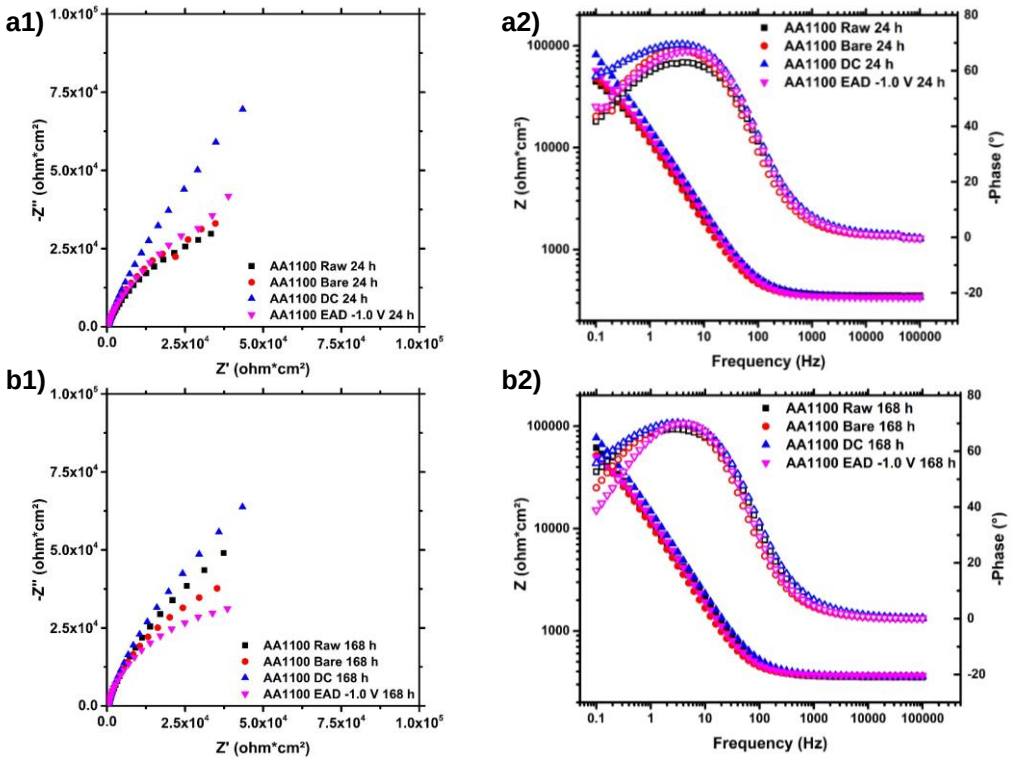

Figure S3. Nyquist (1) and Bode (2) diagrams obtained from electrochemical impedance spectroscopy tests of AA1100 pre-treated samples, after: a) 24 h and b) 168 h of exposure to the electrolyte solution.

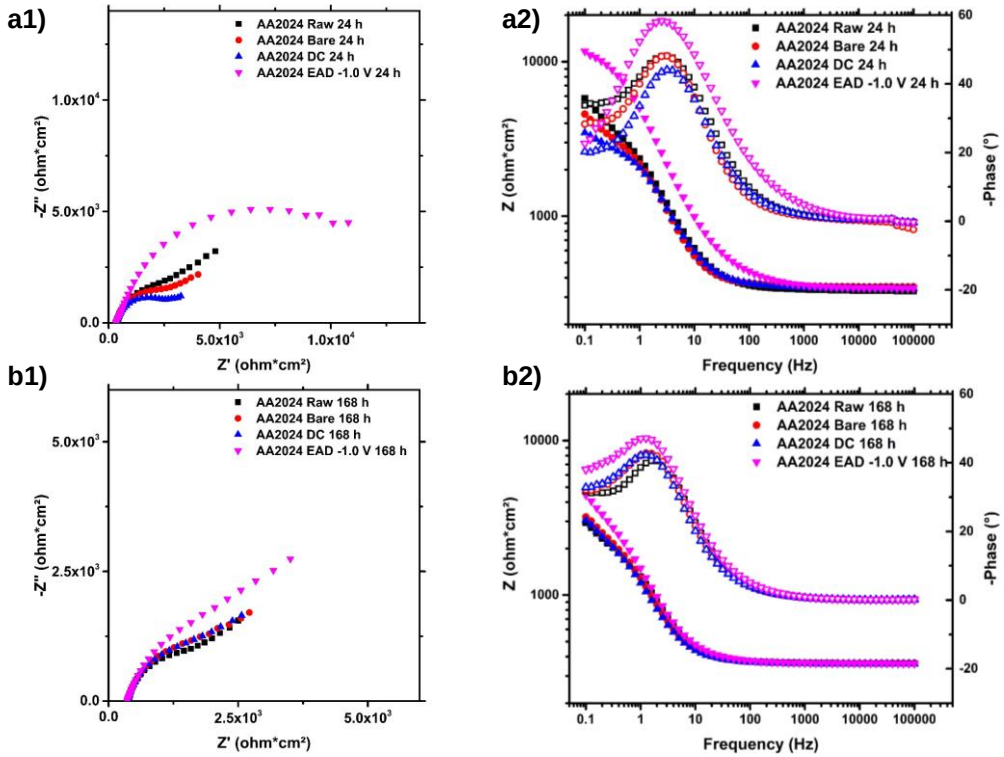

Figure S4. Nyquist (1) and Bode (2) diagrams obtained from electrochemical impedance spectroscopy tests of AA2024 pre-treated samples after: a) 24 h and b) 168 h of exposure to the electrolyte solution.

The plots for impedance module (|Z|) at 0.1 Hz comparison between the studied pretreatments are shown in Figure S5.

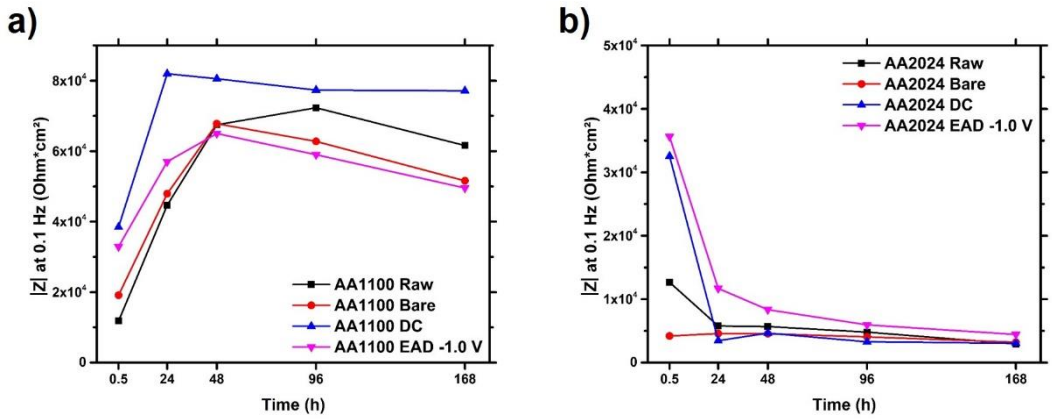

Figure S5. Impedance modules |Z| at 0.1 Hz, measured through electrochemical impedance spectroscopy, from 0.5 to 168 hours of immersion in NaCl 0.05 M solution: a) AA1100 and b) AA2024 substrates, with different pre-treatments.

A general trend of increase in |Z| is visible for all the surface treatments on AA1100 samples (Figure S5a), with the dip-coated sample (DC) having the highest impedance value during the entire test and maintaining almost constant over time. All other substrates

exhibited a fast raise in |Z| modulus at first 48 h of immersion in aggressive solution, but their impedance values become instable after this time. The fact that the impedance module increases during the exposure to the electrolyte in both coated and non-coated samples evidences the self-healing behavior of such oxides in the protection of the metal surface. However, the instability of the oxide nanocoatings leads to a rapid penetration of chlorine ions, destroying the pseudo-barrier protection achieved at short immersion times.

On the other hand, in AA2024 (Figure S5b) a general trend of decrease was observed during the test. Meanwhile, the ZrO_2 generated by EAD method had a smooth decay if compared to the other substrates, showing a better coating resistance in NaCl solution for the analysed period. Both samples coated with ZrO_2 presents a good impedance value at very short exposure time (0.5 h). The Zr-EAD treatment had the highest |Z| during the entire test. Generally, the sharp decrease in |Z| modulus is most likely a consequence of the presence of intermetallic particles in AA2024 surface. After 168 hours of test, EAD resulted in 4449 ohm·cm² and the other treatments' impedances were within the range between 2900 and 3100 ohm·cm².

Figure S6 contains the photographs of one representative specimen of each treatment used for accelerated corrosion testing.

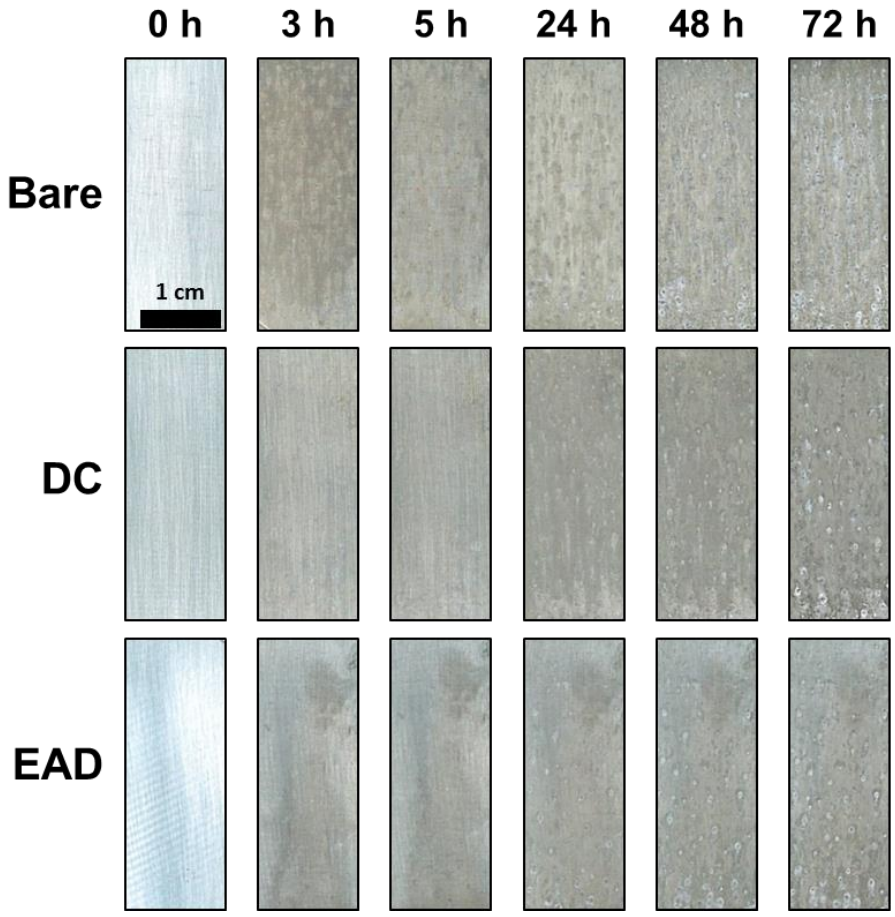

Figure S6. Photographs of AA2024 specimens submitted to cyclic accelerated corrosion test during 72 hours. The scale bar applies to all images.

3.3. Evaluation of the dual protected aluminum substrates under prolonged exposition to NaCl solution

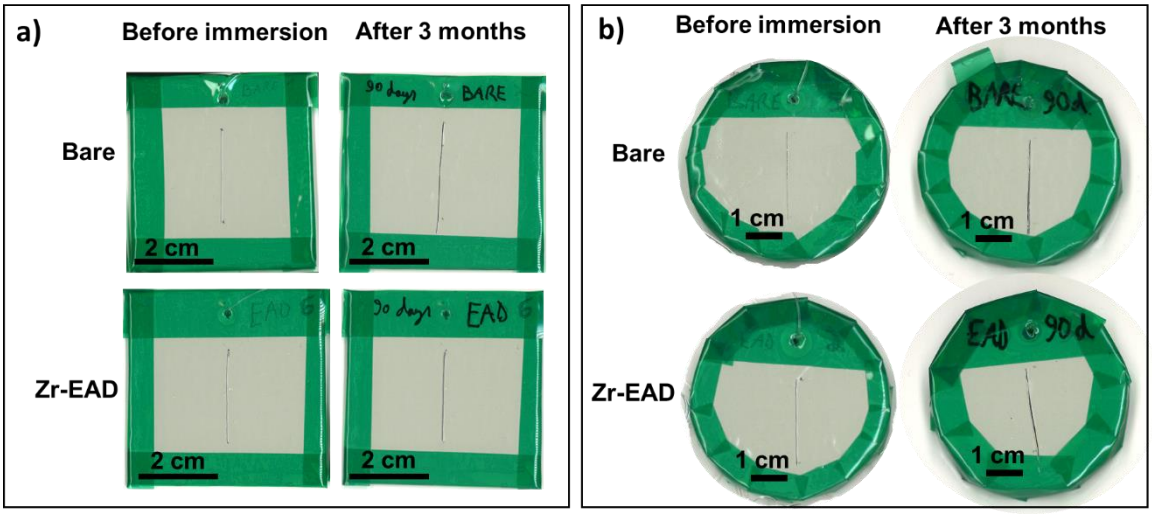

Figure S7. Digital photographs of AA1100 plates (a) and AA2024 discs (b), before and after 90 days of accelerated corrosion assays (NaCl 3.5 wt.%).

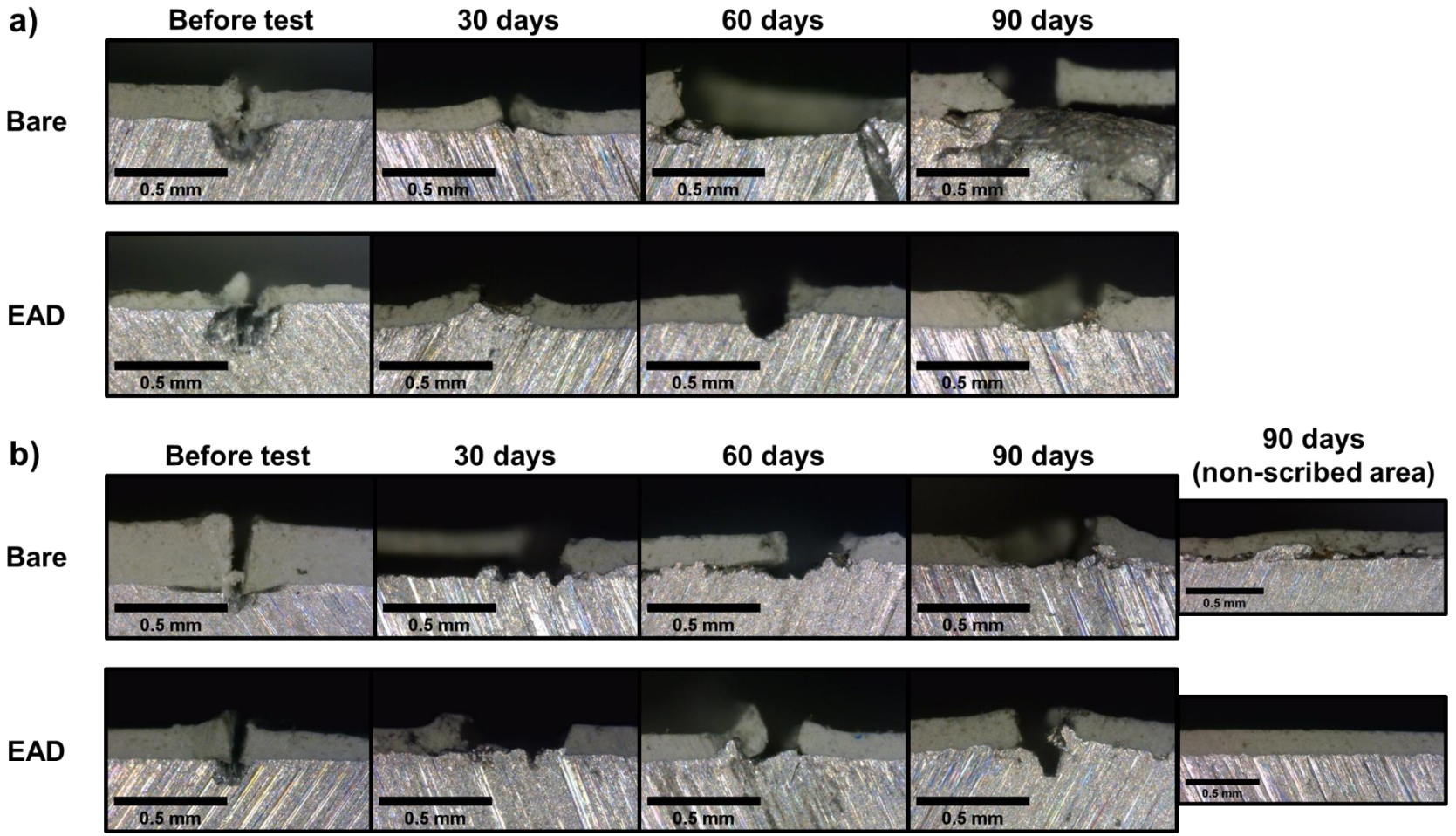

Figure S8. Optical microscopy images of the cross-section of scribed areas in: a) AA1100 and b) AA2024 specimens, submitted to accelerated corrosion test during 90 days.